



HAL
open science

Hydrophobic Collapse of the Intrinsically Disordered Transcription Factor Myc Associated Factor X

Gönül Kizilsavas, Karin Ledolter, Dennis Kurzbach

► **To cite this version:**

Gönül Kizilsavas, Karin Ledolter, Dennis Kurzbach. Hydrophobic Collapse of the Intrinsically Disordered Transcription Factor Myc Associated Factor X. *Biochemistry*, 2017, 56 (40), pp.5365-5372. 10.1021/acs.biochem.7b00679 . hal-01615250

HAL Id: hal-01615250

<https://hal.sorbonne-universite.fr/hal-01615250>

Submitted on 12 Oct 2017

HAL is a multi-disciplinary open access archive for the deposit and dissemination of scientific research documents, whether they are published or not. The documents may come from teaching and research institutions in France or abroad, or from public or private research centers.

L'archive ouverte pluridisciplinaire **HAL**, est destinée au dépôt et à la diffusion de documents scientifiques de niveau recherche, publiés ou non, émanant des établissements d'enseignement et de recherche français ou étrangers, des laboratoires publics ou privés.

Hydrophobic Collapse of the Intrinsically Disordered Transcription Factor MAX

Gönül Kizilsavas, Karin Ledolter, and Dennis Kurzbach

Biochemistry, **Just Accepted Manuscript** • DOI: 10.1021/acs.biochem.7b00679 • Publication Date (Web): 07 Sep 2017

Downloaded from <http://pubs.acs.org> on September 8, 2017

Just Accepted

“Just Accepted” manuscripts have been peer-reviewed and accepted for publication. They are posted online prior to technical editing, formatting for publication and author proofing. The American Chemical Society provides “Just Accepted” as a free service to the research community to expedite the dissemination of scientific material as soon as possible after acceptance. “Just Accepted” manuscripts appear in full in PDF format accompanied by an HTML abstract. “Just Accepted” manuscripts have been fully peer reviewed, but should not be considered the official version of record. They are accessible to all readers and citable by the Digital Object Identifier (DOI®). “Just Accepted” is an optional service offered to authors. Therefore, the “Just Accepted” Web site may not include all articles that will be published in the journal. After a manuscript is technically edited and formatted, it will be removed from the “Just Accepted” Web site and published as an ASAP article. Note that technical editing may introduce minor changes to the manuscript text and/or graphics which could affect content, and all legal disclaimers and ethical guidelines that apply to the journal pertain. ACS cannot be held responsible for errors or consequences arising from the use of information contained in these “Just Accepted” manuscripts.



Hydrophobic Collapse of the Intrinsically Disordered Transcription Factor MAX

Gönül Kizilsavas^{a,‡}, Karin Ledolter^{b,‡} and Dennis Kurzbach^{c,d,*}

^a Max Planck Institute for Polymer Research, Ackermannweg 10, 55128 Mainz, Germany

^b University Vienna, Department for Structural and Computational Biology, Max F. Perutz Laboratories, Campus Vienna BioCenter 5, 1030 Vienna, Austria

^c Département de Chimie, Ecole Normale Supérieure, PSL Research University, UPMC Univ Paris 06, CNRS, Laboratoire des Biomolécules (LBM), 24 rue Lhomond, 75005 Paris, France

^d Sorbonne Universités, UPMC Univ Paris 06, Ecole Normale Supérieure, CNRS, Laboratoire des Biomolécules (LBM), Paris, France

*corresponding author: DK, email: kurzbach@ens.fr, phone: +33 1 44323265

1
2
3 ABSTRACT The conformational space of the proto-oncogenic transcription factor MAX (Myc
4 associated factor X) comprises a dynamic equilibrium between a stably folded coiled-coil
5 homodimer and an intrinsically disordered ensemble of states. We show by means of nuclear
6 magnetic resonance spectroscopy that the intrinsically disordered ensemble samples structures
7 that are even as compact as the folded dimer. These extremely dense, hydrophobically collapsed
8 globules might be of importance for interconversion between different conformations of
9 intrinsically disordered proteins.
10
11
12
13
14
15
16
17
18
19
20
21

22 KEYWORDS Intrinsically Disordered Proteins, NMR, Paramagnetic Relaxation Enhancement,
23
24 Polymer Models, Collapsed Globule.
25
26
27
28
29
30
31
32
33
34
35
36
37
38
39
40
41
42
43
44
45
46
47
48
49
50
51
52
53
54
55
56
57
58
59
60

1
2
3 INTRODUCTION
4

5
6 The MYC-associated factor X (MAX) is a proto-oncogenic transcription factor that
7
8 heterodimerizes with its partner protein MYC to develop transcriptional activity.¹⁻² MYC and
9
10 MAX are driving forces in almost all human cancers as they regulate the transcription of proteins
11
12 involved in DNA replication and cell proliferation and are therefore involved in high activity.³
13
14 For both, MYC and MAX the central structural element is a basic/helix-loop-helix/leucine zipper
15
16 (b/H₁LH₂/LZ) conformation⁴⁻⁵ - a motif that is also found important for MYC:MAX
17
18 heterodimerization.
19
20
21
22

23
24 In the absence of MYC, MAX populates a heterogeneous conformational space including
25
26 intrinsically disordered conformations as well as a stably folded coiled-coil homodimer that
27
28 adopts the b/H₁LH₂/LZ conformation.⁶ The dynamic sampling of such heterogeneous
29
30 conformational spaces includes often the transient population of conformations that are devoid of
31
32 any secondary or tertiary structure elements, but show varying compactness along the
33
34 polypeptide chain.⁷⁻⁸ Such conformations are frequently involved in substrate interactions
35
36 (conformational selection, entropic compensation) or folding processes where they may act as
37
38 folding nuclei and rate regulating entities.^{7,8} Understanding these states might help to tackle the
39
40 still not resolved problem of protein folding and conformational averaging as well as to elucidate
41
42 the relation between the complicated conformational dynamics of the MYC-MAX proto-
43
44 oncoprotein network and the development of cellular transcriptional activity.
45
46
47
48
49

50
51 We here report by means of nuclear magnetic resonance (NMR) a novel intrinsically disordered
52
53 state of MAX, which features a very high compactness. It can be described as hydrophobically
54
55 collapsed globule of high density comparable to that of the stably folded coiled-coil b/H₁LH₂/LZ
56
57
58
59
60

1
2
3 structure of the homodimer (denoted as MAX₂) in contrast to the monomer (denoted as MAX).
4
5 The described intrinsically disordered state might be of importance for the formation of the
6
7 transcriptionally active MYC:MAX dimer that depends on the concentration of ready-to-react
8
9 monomeric MAX in the cellular environment.
10
11

12 13 MATERIALS/EXPERIMENTAL DETAILS

14 15 16 17 *NMR*

18
19
20 Heteronuclear single quantum coherence (HSQC) spectra were recorded at 35 °C using a
21
22 Varian Direct Drive 800 MHz spectrometers. Spectra were recorded in the States-TPPI/PFG
23
24 sensitivity-enhanced mode for quadrature detection with carrier frequencies for ¹H^N and ¹⁵N of
25
26 4.73 and 120.0 ppm, respectively. The samples contained 1.2 mM MAX, 25 mM MES, and 25
27
28 mM NaCl (pH 5.5) in a 90% H₂O/10% D₂O mixture. Intramolecular paramagnetic relaxation
29
30 enhancement (PRE) of MTSL labeled Cys mutants were carried out in a similar fashion.
31
32 Reference measurements were performed after reduction of the *S*-(1-oxyl-2,2,5,5-tetramethyl-
33
34 2,5-dihydro-1H-pyrrol-3-yl)methyl methanesulfonylthioate (MTSL) label with an excess of
35
36 ascorbic acid.
37
38
39
40
41

42
43 All NMR spectra were processed and analyzed using NMRPipe, SPARKY and home-written
44
45 scripts based on the MATLAB program package. A squared and 60° phase-shifted sine bell
46
47 window function was applied in all dimensions for apodization. Time domain data were zero-
48
49 filled to twice the data set size, prior to Fourier transformation. The applied pulse sequences are
50
51 sensitivity-enhanced and use gradients for coherence selection and water suppression. NMR
52
53 resonance assignment (~80%) was achieved by a combination of several three-dimensional
54
55 techniques (HNN, HN(C)N⁹ and HNCACB¹⁰ spectroscopy.
56
57
58
59
60

Relaxation Measurements.

¹⁵N longitudinal relaxations experiments for evaluating T₁ were performed at 800 MHz Larmor frequency with relaxation delays of 0, 50, 150 and 250 ms using a recycling delay of 2 s.

¹⁵N transverse relaxations experiments for evaluating T₂ were performed at 800 MHz Larmor frequency with relaxation delays of 0, 16, 32, 64, 128, 192, and 256 ms using a recycling delay of 1 s.

In both cases, the sequence of cross-peak intensities in this series of spectra was fitted to a two-parameter exponential decay of the form

$$I(t) = A \exp[-(\tau/T_2)]$$

where $I(t)$ represents the peak intensity and τ the delay time.

Heteronuclear steady-state NOE ¹⁵N{¹H} attenuation factors were derived at 14.1 T from the $\eta = I_{NOE} / I_{REF}$ ratio, where I_{NOE} and I_{REF} denote the peak intensities in the experiments with and without proton saturation. In the case of spectra without saturation, a net relaxation delay of 5 s was employed whereas a relaxation delay of 2 s prior to a 3 s proton presaturation period was applied for the NOE spectra. Acquisition parameters were identical to those of the PFG sensitivity-enhanced 2D ¹H-¹⁵N HSQC experiments.

Reference PRE Measurements

Intermolecular paramagnetic relaxation enhancement (PRE) reference measurements were carried out at different concentrations between starting from 0.2 mM wt-¹⁵N-MAX + 0.2 mM MTSL-labeled ¹⁴N-MAX to 0.4 mM wt-¹⁵N-MAX + 0.4 mM MTSL-labeled ¹⁴N-MAX (mutants

1
2
3 R5C, G35C and R55C) using the HSQC method as indicated above. Likewise reference
4
5 measurements were carried out with 1 mM Mn²⁺·EDTA or in the presence of 1 mM free MTSL
6
7 in the solution.
8
9

10 11 *Calculation of PRE rates*

12
13
14 As pointed out by Wagner and co-workers, the intensity ratio V between oxidized and reduced
15
16 state of an MTSL label of a protein sample can be expressed as:¹⁴
17
18

$$19 \quad V = R_2 \exp(-\Gamma_2 t) / (R_2 + \Gamma_2) \quad (1)$$

20
21
22 Where Γ_2 denotes the PRE rate and R_2 the intrinsic relaxation rate (absence of spin label) of any
23
24 ¹H^N nucleus. t denotes the time that the proton magnetization is transverse through the HSQC
25
26 experiment (9 ms). Assuming a simple spherical motion with a single correlation time τ_e the PRE
27
28 rate is given by:¹⁵
29
30
31
32

$$33 \quad \Gamma_2 = 1/15(\mu_0\gamma_{\text{HG}}\mu_{\text{B}}/4\pi)2S(S+1)[4J(0)+3J(\omega_{\text{L}})]\langle r^{-6} \rangle \quad (2)$$

34
35
36
37
38 with

$$39 \quad J(\omega) = \tau_e / (1 + \omega^2 \tau_e^2) \quad (3)$$

40
41
42 ω_{L} denotes the Larmor frequency of the proton. S denotes the electron spin number. All other
43
44 symbols have their usual meaning. The average distance, $\langle r \rangle$, between the unpaired electron and
45
46 the nucleus of interest corresponds to the average distance, $\langle R \rangle$, in eq. 5, obtained from the
47
48 Flory-type collapsed globule model. Thus, by choosing N in eq. 5 corresponding to the number
49
50 of residues between the unpaired electron and the amide proton under consideration we can
51
52 calculate the residue dependence of the PRE rate for a hydrophobically collapsed coil.
53
54
55
56
57
58
59
60

Note that the assumption of a single correlation time is most-likely an oversimplification of the model, but here suffices to reproduce the experimentally observed PRE profiles.

DOSY

DOSY was measured on an 800 MHz Bruker HD III spectrometer equipped with a BCU II variable temperature unit using a Z-gradient 5 mm BBO probe. The pulse sequence and analysis method proposed by Wilkins et al.¹⁶ (supplemented with a WATERGATE element to suppress the water signal) was used employing a 128-increment linear gradient profile. The data was processed and fitted using the DOSY toolbox.¹⁷ In a 500 mL sample of 0.4 mM concentration 5 μ L 2,4 dioxane were added as internal standard. Data for the disordered state were recorded at 35 °C and pH 5.5. Data for the folded state were recorded at 20 °C and pH 5.5.⁶

CPMG RD

Carr-Purcell-Meiboom-Gill (CPMG) relaxation dispersion (RD) NMR data were measured as suggested by Kay and co-workers¹¹ at 35 °C at 600 and 800 MHz proton Larmor frequency at CPMG frequencies, ν_{CPMG} , of 33, 67, 133, 167, 266, 333, 400, 467, 533, 600 and 667 Hz. The recycling delay was 1 s. The measured effective relaxation rates, $R_{2,\text{eff}}$, were fitted globally (considering all residues that showed relaxation dispersion) to the general two side exchange model of Carver and Richards assuming that $R_{2,0}$ is equal for both states A and B :

$$R_{2,\text{eff}}(\nu_{\text{CPMG}}) = 0.5 \{ (R_{2,0} + k_{\text{ex}} - \tau_{\text{cp}}^{-1}) \operatorname{acosh}[D_+ \cosh(\eta_+) - D_- \cos(\eta_-)] \}$$

$$D_{\pm} = 0.5 \{ \pm 1 + (\psi + 2(\delta\omega)^2) / [\psi^2 + (2\delta\omega(p_A - p_B) k_{\text{ex}})^2]^{1/2} \}$$

$$\eta_{\pm} = \tau_{\text{cp}} / \sqrt{2} \{ \pm \psi + [\psi^2 + (2\delta\omega(p_A - p_B) k_{\text{ex}})^2]^{1/2} \}^{1/2}$$

$$\psi = [(p_A - p_B) k_{ex}]^2 - (\delta\omega)^2 + 4p_A p_B k_{ex}^2 \quad (4)$$

p_A and p_B denote the populations of states A and B. $R_{2,0} = 1/T_{2,0}$ denotes the relaxation rate in the absence of exchange.

TRACT

TRACT experiments were performed and analyzed as suggested in reference ¹⁸ at 18.8 T magnetic field strength at 35 °C.

Protein Expression and Purification

MAX was subcloned into a Pet3d expression vector and transformed into E.coli BL21 pLysS cells. Cells were grown at 37°C in M9 (for ¹³C and ¹⁵N labeling; 1 g/L ¹⁵N ammonium chloride; 3 g/L ¹³C glucose) and induced at an A600 nm of 0.5 with 0.5 mM IPTG at 30 °C over night. Cell pellets were homogenized in 20 mM PBS, 100 mM NaCl and 1 mM EDTA. For protein purification, fractional NH₄SO₄ precipitation (50% and 80% saturation) was carried out and anion exchange chromatography was applied. The final total protein concentration was 0.4 mM except for intermolecular reference measurements where concentrations up to 0.8 mM were tested to assure the absence of any intermolecular PREs.

Cysteine mutants and MTSL (S-(1-oxyl-2,2,5,5-tetramethyl-2,5-dihydro-1H-pyrrol-3-yl)methylmethanesulfonothioate) labeled proteins were produced according to methods published earlier.¹⁹⁻²⁰ Excess spin label was removed by dialysis into the buffer used for the NMR experiments. PRE referencing was achieved by reduction of the MTSL label through incubation for 1 h with tenfold excess of ascorbic acid at 35 °C.

1
2
3
4
5
6
7 RESULTS AND DISCUSSION
8
9

10 Fig. 1a shows the structural motifs of the primary sequence of MAX₂. Each unit of the
11 homodimer can be separated into a rather flexible basic N-terminal domain (NTD) between
12 amino acid (aa) 1 and 16, which houses the primary DNA recognition motif and a very rigid
13 H₁LH₂/LZ segment located between aa 16 and 82.
14
15
16
17
18
19
20
21
22
23
24
25
26
27
28
29
30
31
32
33
34
35
36
37
38
39
40
41
42
43
44
45
46
47
48
49
50
51
52
53
54
55
56
57
58
59
60

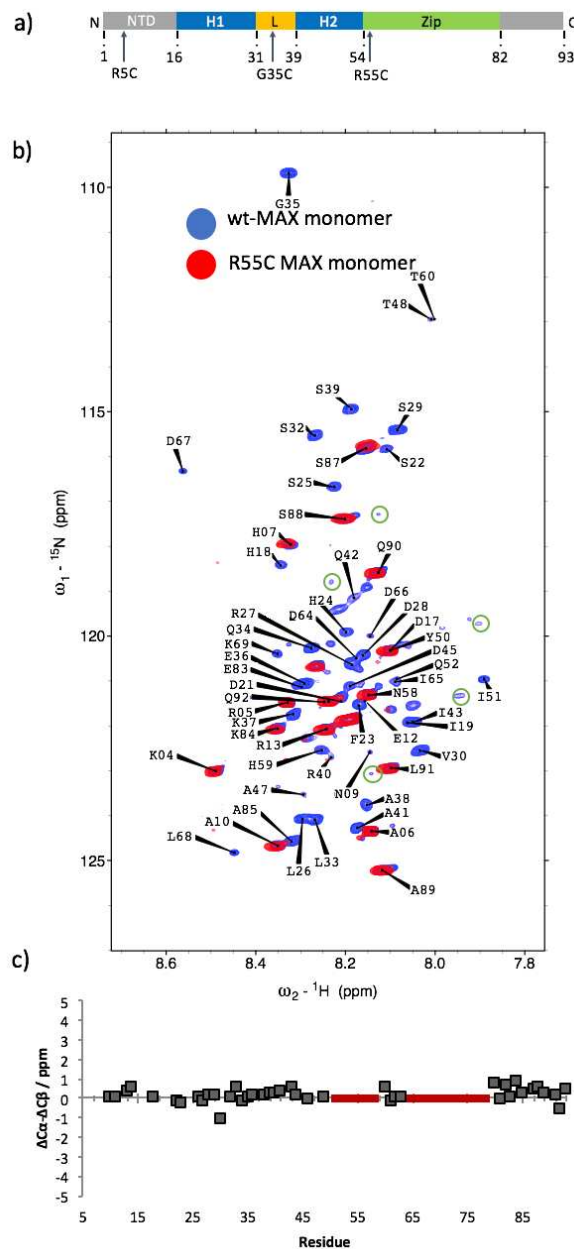


Figure 1. a) Schematic display of the structural constitution of a MAX₂ unit. The MTSL labeling sites R5, G35 and R55 employed here are indicated. b) ¹H-¹⁵N 2D correlation NMR spectrum (HSQC) of the MAX monomer (blue) and of a spin labeled mutant (red) of the monomeric form. The amino acid assignment is indicated. A tabular form can be found in the Supporting Information. The green circles exemplarily indicate residues that could not be assigned due to

1
2
3 weak signal intensities (see text). c) ^{13}C secondary chemical shifts found for the MAX monomer.
4
5
6 The red bar indicates stretches of not assigned residues.
7

8
9 For the study at hand, we chose experimental conditions of pH 5.5 and a temperature of 35 °C.
10
11 Under these conditions, MAX₂ dissociates and the protein almost entirely populates a
12 monomeric, intrinsically disordered state.⁶ Such, conditions are relevant as MAX is residing
13 close to DNA strings in the cellular environment, where pH values can drastically drop as
14 compared to a physiological pH of 7.4.²¹ Fig. 1b shows a ^1H - ^{15}N 2D correlation NMR spectrum
15 (heteronuclear single quantum coherence; HSQC) of the MAX monomer (blue). The chemical
16 shift dispersion in the proton dimension is very low as expected for an intrinsically disordered
17 protein (IDP). The lack of secondary or tertiary structure elements is further corroborated by
18 residue resolved ^{13}C NMR secondary chemical shifts (Fig. 1c) – considered as deviation of $\text{C}\alpha$
19 and $\text{C}\beta$ chemical shifts from values predicted for random coils (denoted $\Delta\delta$).¹⁰ These shifts
20 ($|\Delta\delta(\text{C}\alpha)| - |\Delta\delta(\text{C}\beta)|$) are found to be close to zero throughout the entire primary sequence
21 indicating the absence of any significant structural propensities in the MAX monomer, which
22 would entail noteworthy deviations from zero.¹⁰ For the folded homodimer, strong positive shifts
23 ($\Delta\delta(\text{C}\alpha) - \Delta\delta(\text{C}\beta) > 0$) were observed in earlier studies⁴ between aa 16 and 82 corresponding to
24 the α -helical elements in the H₁LH₂/LZ domain (see Fig. 2 for the structure of the leucine
25 zipper).⁶
26
27
28
29
30
31
32
33
34
35
36
37
38
39
40
41
42
43
44
45
46
47
48
49
50
51
52
53
54
55
56
57
58
59
60

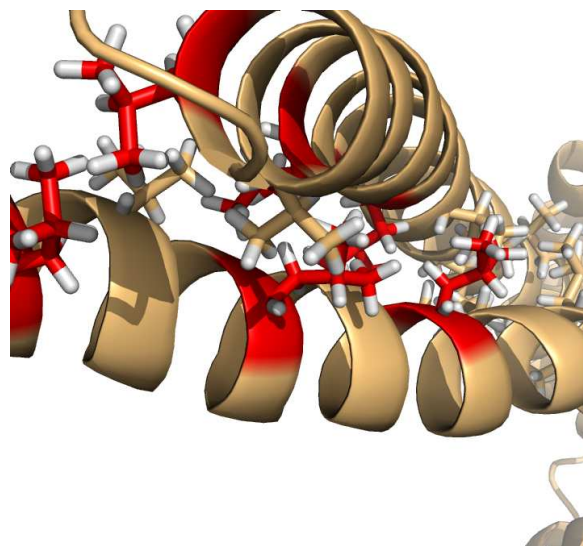


Figure 2. Zoom into the leucine zipper of MAX₂. Hydrophobic side chain contacts guarantee the stability of the coiled-coil motif. Leucine residues are highlighted in red, Leu-attached protons in white.

Interestingly, signal intensities vary significantly between the different cross peaks in the HSQC spectrum in Fig. 1b. This hints towards a relaxation process that reduces the intensity of a subset of the observed NMR signals. Indeed, via relaxation dispersion experiments (see the Supporting Information) we find that MAX undergoes exchange processes with a global frequency of 702 ± 75 Hz that can broaden NMR signals. Unfortunately, for these residues we could not achieve an NMR signal assignment as the corresponding signals were too weak in 3D assignment experiments (especially in HNCA and HNCACB experiments) hampering assignment of (¹³C) chemical shifts. Using the HNN and HN(C)N⁹ experiments this problem could partly be overcome to assign more ¹H^N and ¹⁵N resonances.

To cast light on the properties of the intrinsically disordered (monomeric) form of MAX we employed the paramagnetic relaxation enhancement (PRE) technique. To this end, three unique

1
2
3 MAX cysteine mutants were introduced at positions R5C, G35C and R55C (see Fig. 1a and 3a
4 for a graphical display of these sites within the protein construct). The cysteine residues were
5 subsequently labeled with the paramagnetic spin label MTSL (see the Experimental section for
6 details). Short distances between a spin labeled residue and any other amino acid of a protein
7 reduces the amino acid's NMR signal intensity through line broadening. Corresponding signals
8 in the ^1H - ^{15}N 2D NMR correlation spectra are thus attenuated (cf. Fig. 1b). Signals in direct
9 vicinity of an MTSL label are normally even broadened beyond the detection threshold. Long-
10 range PREs, remote to a labeling site, typically stem from compacted conformations that reduce
11 the average distance, $\langle r \rangle$, between the nucleus of interest and the unpaired electron as the effect
12 depends very steeply on the distance by r^{-6} .¹⁵ Contributions of elongated conformations are, thus,
13 effectively invisible by means of PRE. Fig. 3b indicates the residue-resolved signal reduction.
14 This signal reduction is determined via the ratio, $V = I / I_0$, with I being the signal intensity
15 observed with the active spin label (blue in Fig. 1b), and I_0 being the signal intensity with a
16 deactivated (chemically reduced with ascorbic acid) label (red in Fig. 1b). For the labeling site
17 R5C located in the basic NTD of MAX one observes strong effects ($V \ll 1$) around the labeling
18 site (short-range PRE), but only minor ($V < 1$) or no PREs for the rest of the primary sequence
19 (long-range PRE). In stark contrast, for labeling sites G35C and R55C around 70-80 % of the
20 NMR signals of the central part of the primary sequence are broadened beyond detection (long-
21 range PRE; $V \ll 1$). To the best of our knowledge such a pronounced PRE effect has not been
22 observed so far for any protein, neither for disordered nor for folded ones. The suppression of
23 most of the NMR resonances, as observed for mutants G35C and R55C, indicates a very dense
24 state of between aa 20 and 85 (corresponding to the H₁LH₂/LZ domain) of disordered MAX
25
26
27
28
29
30
31
32
33
34
35
36
37
38
39
40
41
42
43
44
45
46
47
48
49
50
51
52
53
54
55
56
57
58
59
60

which implies close proximity between these residues and the MTSL label. In contrast, the basic NTD remains elongated.

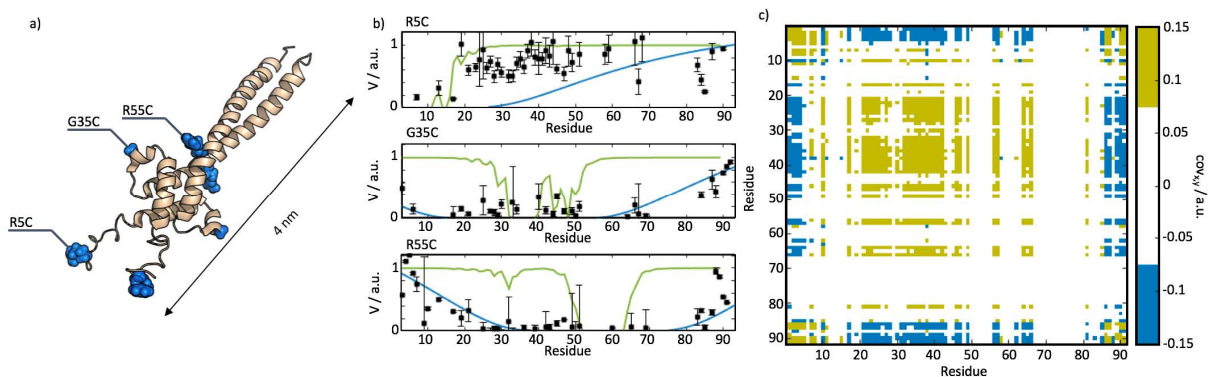


Figure 3. a) NMR solution structure of the MAX₂ homodimer. MTSL labeled residues are highlighted in blue. b) Residue plots of the intensity ratios, V , obtained for the three labeling sites in the disordered monomeric state of MAX (black squares). PRE ratios expected for the folded NMR solution structure of the homodimer are shown as green line. PRE ratios expected for a collapsed globule-like conformation are shown as blue line. c) Covariance matrix calculated from the PRE data in b), according to reference 28. Green matrix elements correspond to positive matrix elements, blue to negative elements.

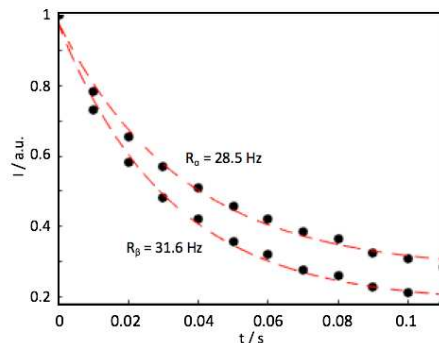
The collapse of the MAX monomer can be rationalized when considering the physics of the hydrophobic collapse of a polymer in a poor solvent. In the framework of scaling laws for IDPs as pioneered by Schuler and co-workers²²⁻²⁴ the average distance, R , between two residues separated by N residues in such a hydrophobically collapsed coil-like state is given by

$$\langle R \rangle = |v|^{-1/3} b^2 N^{1/3} \quad (5)$$

1
2
3 , with a Flory-type scaling exponent of $1/3$.²⁵ v is the excluded volume, b denotes the average
4 amino acid diameter (ca. 0.23 nm). The scaling exponent of $1/3$ corresponds to a state of
5 maximal compactness of a random walk-type polypeptide chain²⁵ and is here, to the best of our
6 knowledge, reported for the first time for a protein.
7
8
9
10
11

12
13
14 The blue line in Fig. 3b indicates the PRE-intensity ratios, V , that one would expect for the
15 different residues of MAX in a state of full hydrophobic collapse according to eq. 5. The
16 theoretical PRE profiles were calculated by assuming that $\langle r \rangle = \langle R \rangle$ (the average distance
17 between the amino acid and the radical (as relevant for PRE) equals the average distance
18 between two residues in the collapsed globule model). Additionally, we postulated an average
19 global rotational correlation time τ_c of the vectors connecting the labeling site (position 5, 35 or
20 55) and the amino acids in the MAX backbone for the calculation (considering references¹⁴⁻¹⁵
21 and equations therein; see the Methods section for details). Note that the rotational correlation
22 time and the excluded volume are the only two variables that determine the shape of the PRE
23 profile calculated for the collapsed globule (cf. Fig. 3b) and that they are correlated and cannot
24 be determined independently. In other words, a similar profile could be obtained with a longer τ_c
25 and a larger v or *vice versa*. For an IDP of 93 residues like MAX one may roughly anticipate
26 rotational correlation times of $1 \text{ ns} < \tau_c < 4 \text{ ns}$.^{10, 26-27} To reproduce the data in Fig. 3b for this
27 range of τ_c the corresponding excluded volumes varies between -0.12 nm^3 and -0.15 nm^3 .
28
29 Assuming a rigid body spherical spectral density function, we find an average rotational
30 correlation time of $1.6 \pm 0.4 \text{ ns}$ via TRACT (TROSY for rotational correlation times)
31 measurements (see Fig. 4) according to reference¹⁸ under the assumption of a hard sphere model
32 and a single rotational correlation time. Yet, we want to stress that such an assumption and the
33 corresponding spectral density function of the form $J(\omega) = \tau_c / (1 + \omega^2 \tau_c^2)$ is an oversimplification
34
35
36
37
38
39
40
41
42
43
44
45
46
47
48
49
50
51
52
53
54
55
56
57
58
59
60

1
2
3 that might yield substantial systematic errors. The value for the rotational correlation time is thus
4
5 only a rough estimate of the effective average correlation time.
6
7
8
9



10
11
12
13
14
15
16
17
18
19
20
21
22
23 **Figure 4.** TRACT time traces and corresponding fits. The decay rates for the α and β spin states
24 are indicated in the figure for MAX at 35 °C and 18.8 T.
25
26
27
28

29 Similar words of caution should be considered when calculating the theoretical PRE profiles in
30 Fig. 3b.
31
32

33
34 For Fig. 3b we exemplarily assumed an excluded volume of -0.13 nm^3 and a τ_c of 1.6 ns. With
35 these two parameters and the model of a collapsed globule we can reproduce the experimental
36 PREs found for labeling sites G35C and R55C as obvious from the correspondence of the blue
37 reproduction line and the experimental data points. However, with our polymer physical model
38 we cannot reproduce the effect of the MTSL label at position R5C, which is placed in the
39 hydrophilic NTD, and does not take part in the formation of the hydrophobic core, but remains
40 solvent exposed.
41
42
43
44
45
46
47
48
49
50

51
52 Fig. 3b shows in green PREs expected for distances extracted from the NMR-derived solution
53 structure⁴ of the folded dimeric form, MAX₂. The folded solution structure resembles the crystal
54 structure⁵ of the homodimer indicating the high stability and rigidity of this complex. Strikingly,
55
56
57
58
59
60

1
2
3 the folded dimer shows a narrower dispersion of PREs around the labeling sites G35C and R55C
4
5 than the disordered state. In other words, the unfolded state appears more compact than the
6
7 folded state in our PRE measurements.
8
9

10
11 To rationalize this finding, we consider that the diameter along the main symmetry axis of MAX₂
12
13 indicated in Fig 3a is about 4 nm. For the collapsed globule model, we would expect a diameter
14
15 between 1.7 nm and 2.1 nm, according to eq. 5, depending on the extend of the excluded volume
16
17 of $-0.12 \text{ nm}^3 < v < -0.15 \text{ nm}^3$.²⁵ The collapsed globule can be described by a three-dimensional
18
19 random walk with maximum packing density with all water molecules being expelled from the
20
21 hydrophobic core and strong intramolecular attraction. It is thus possible to obtain a structure
22
23 that is even more compressed than a (classically) folded conformation as the latter might feature
24
25 more void spaces, extended loops and enclosed solvent molecules. In the case of the coiled-coil
26
27 MAX₂ - a structure that is asymmetrically elongated - the larger expansion in one direction of
28
29 space in comparison to the compressed globular state of the monomer will lead to larger
30
31 distances between the labeling sites G35C and R55C and the other amino acids in the backbone
32
33 of the IDP.
34
35
36
37
38
39

40
41 Summing up, the PRE profiles displayed in Fig. 3b indicate an extended, disordered basic NTD
42
43 and a densely collapsed globule for the rest of the monomeric form of MAX. This distinction
44
45 between NTD and the rest of the protein is further corroborated by a covariance analysis of our
46
47 PRE data. This was performed as demonstrated in detail in reference 28 and the result is shown
48
49 in Fig. 3c. We compute covariance matrix elements between pairs of residues from the three
50
51 PRE data sets (labeling sites) such that the resulting matrix has the dimension and order of the
52
53 primary sequence of MAX. Positive matrix elements indicate pairs of residues that are correlated
54
55 in the formation of the compacted state, while negative elements indicate residues that are
56
57
58
59
60

1
2
3 excluded from the compact conformation. The matrix displays a strongly correlated patch
4
5 between residues 20 and 85 indicating that these residues collectively take part (i.e., they are
6
7 correlated) in the formation of a compacted state that embraces the entire H₁LH₂/LZ segment. In
8
9 contrast, the NTD (and the C-terminus) are anti-correlated to this region. In other words, they are
10
11 not partaking in the formation of the hydrophobic core, but are expelled from this compacted
12
13 region and remain solvent exposed. Considering the hydrophobic residues that form the internal
14
15 surface of the coiled-coil motif in the dimer (Fig. 2), a picture arises in which these residues
16
17 cluster in the core of the collapsed globule expelling all hydration water from its core, while this
18
19 state is stabilized in the aqueous environment by MAX's hydrophilic residues comprised in the
20
21 basic NTD and the C-terminal region of the primary sequence.
22
23
24
25
26
27

28 Note that the experimentally observed PRE profiles could be constituted by a single collapsed
29
30 conformation or by an ensemble of structures for which we would observe an ensemble-average
31
32 in our PRE measurements. *A priori*, the polymer physical description of a collapsed globule does
33
34 not exclude the formation of different sub-states, instead it describes the ensemble average
35
36 distance considering all the possible conformations of the polypeptide chain in a poor solvent.²⁵
37
38 In the latter case the abovementioned diameters between 1.7 nm and 2.1 nm should be regarded
39
40 as ensemble averaged values.
41
42
43
44

45 Yet, to verify the observation of a highly compressed disordered state of MAX we performed
46
47 PFG-DOSY (pulse field gradient - diffusion ordered spectroscopy) NMR measurements
48
49 according to the method proposed by Wilkins et al.¹⁶ The results are shown in Fig. 5 (see the
50
51 Methods section for details). We find a hydrodynamic radius of the folded MAX₂ of $R_h =$
52
53 1.9 ± 0.2 nm (corresponding to a diffusion coefficient, D , of $1.13 \cdot 10^6$ cm²s⁻¹ at 20 °C), which
54
55 corresponds well to the extension of the elongated coiled-coil structure along its principle axis
56
57
58
59
60

(cf. Fig. 3a). For the unfolded state, we find $R_h = 2.3 \pm 0.3$ nm (corresponding to a diffusion coefficient, D , of $1.31 \cdot 10^6$ cm²s⁻¹ at 35 °C). The hydrodynamic radius of the unfolded conformation is thus within the error margin, similar to the radius of the folded state, indicating the presence of a compacted sub-ensemble that reduces the ensemble-averaged hydrodynamic radius of the disordered state. In contrast, one would anticipate an R_h of 2.9 nm for a completely unfolded protein (e.g., in a solution of 8 M urea) of the length of MAX according to empirical relations as described in reference 16 highlighting the here reported compactness of the conformational ensemble of MAX.

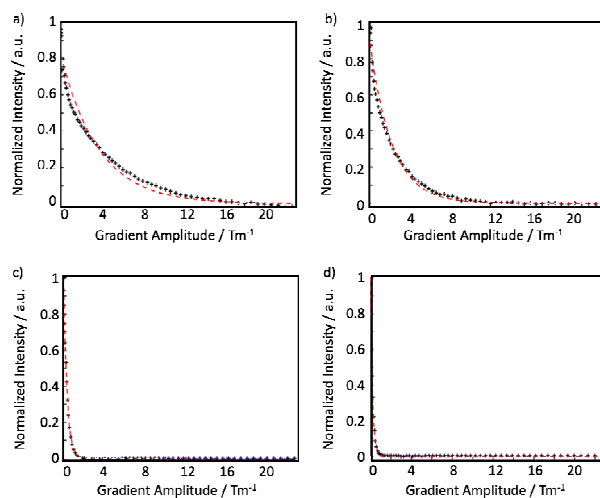


Figure 5. a) DOSY decay trace for MAX₂ at 20 °C. The red solid line was fitted to the data as a monoexponential function. b) DOSY decay trace for 2,4-dioxane at 20 °C. c) DOSY decay trace for MAX at 35 °C. d) DOSY decay trace for 2,4-dioxane at 35 °C.

Comparing the hydrodynamic radii found for the folded state (1.9 ± 0.2 nm), the disordered ensemble (2.3 ± 0.3 nm) and anticipated for the entirely unfolded state (2.9 nm)¹⁶ we deduce that the intrinsically disordered state of MAX cannot be described by an ideal random coil picture as it is on average more compact than the hypothetically completely unfolded state. From

1
2
3 theoretical considerations one would expect a Flory scaling exponent of 0.588 for this case with
4 aqueous buffers considered as good solvents for urea denatured proteins. This expansion would
5 entail an increased R_h , which is reflected in a larger average end-to-end distance in the polymer
6 physical description. Indeed, one would find $\langle R \rangle = b(v/b^3)^{0.18} N^{0.588}$ to describe an unstructured
7 coil in a good solvent, i.e., with stabilizing interactions between the solvent and polypeptide (cf.
8 eq. 5, where we find $N^{1/3}$ to describe the reduced coil expansion).²⁵ Yet, the high degree of
9 compactness of the collapsed globule must be considered to understand the smaller
10 hydrodynamic radius of the intrinsically disordered state as the buffer becomes poor solvent for
11 the hydrophobic amino acids of MAX in the absence of a denaturation agent such that the
12 intramolecular attractions become stronger than the stabilizing interaction with the solvent.
13 These findings are in line with the recent insights that IDPs cannot simply be considered as
14 unfolded polypeptide chains, but instead sample heterogeneous conformational spaces that
15 contain conformations that can deviate from the simple picture of random coils.²⁹ To this picture
16 we add here another state of possible conformations of IDPs, which comprises an unusually high
17 compactness despite the absence of any secondary or tertiary structure motifs.

18
19
20 Note that we carefully excluded intermolecular interactions that can bias the PRE measurements
21 by performing experiments on a mixture of ^{15}N -labeled (but not spin-labeled) wildtype (wt)
22 MAX and ^{14}N and spin-labeled MAX (mutants R5C, G35C and R55C; see the Supporting
23 Information). In none of these experiments we detected any significant intermolecular PRE
24 under our experimental conditions. Additionally, solvent PREs due to the presence of
25 paramagnetic salts or free MTSL present in the solution have been excluded.

These results are shown in the Supporting Information. No significant intermolecular PRE can be detected. Likewise, no PRE effect was detected in the presence of 1 mM Mn^{2+} ·EDTA or in the presence of 1 mM free MTSL in the solution.

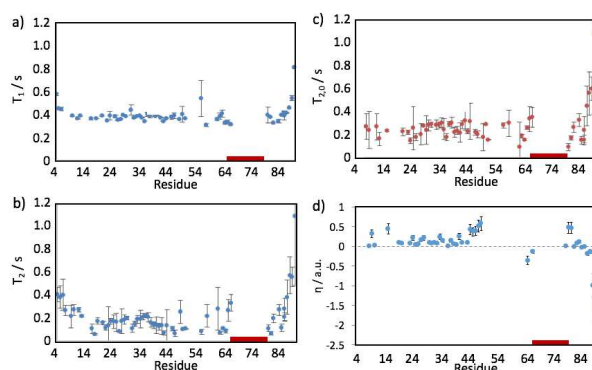


Figure 6. a) Residue-resolved ^{15}N - T_1 values for the monomeric form of MAX at 35°C and 18.8 T (800 MHz). The red bar indicates a patch of residues that could not be assigned due to weak signal intensities. b) Residue-resolved ^{15}N - T_2 values for the monomeric form of MAX at 35°C and 18.8 T (800 MHz). c) T_2 values detected with a CPMG field to suppress the exchange contribution (denoted $T_{2,0}$). d) Heteronuclear ^{15}N - $\{^1\text{H}^{\text{N}}\}$ Overhauser enhancement (NOE, η) as a function of residue position obtained at 35°C and a magnetic field of 14.1 T (600 MHz). For some residues, η could not unambiguously determined due to the lower field and signal overlap.

To further characterize the conformational sampling of monomeric MAX, we determined heteronuclear longitudinal ^{15}N - T_1 and transverse ^{15}N - T_2 relaxation times as well as transverse ^{15}N - $T_{2,0}$ times, i.e., ^{15}N - T_2 in the presence of a CPMG field that suppresses exchange

1
2
3 contributions to transverse relaxation (see Fig. 6 a-c). These measurements were performed at
4
5 18.8 T magnetic field strength. Displaying a rather flat profile, the ^{15}N - T_1 data shown in Fig. 6a
6
7 do not indicate significant variations in local backbone flexibility in the central domain between
8
9 aa 20 and 85. Structural elements would cause variations in local backbone dynamics, which in
10
11 return would cause significant fluctuations in the ^{15}N - T_1 values in dependence of the residue
12
13 position. This is not observed here. Only the termini show elevated values due to their
14
15 intrinsically higher mobility. This is in accordance with the above-deduced picture of a collapsed
16
17 random-coil structure between aa 20 and 85 void of any significant structural elements. Under
18
19 our experimental conditions, a short relaxation time generally indicates slow backbone
20
21 dynamics, while a long relaxation indicates the opposite. The average ^{15}N - T_1 value of 0.40 s is
22
23 quite low for an IDP¹⁰ thus suggesting a relatively low conformational flexibility and slow local
24
25 tumbling (on the nanosecond timescale) of residues in the disordered state of MAX, again
26
27 corroborating the idea of a high level of compression due to locally reduced flexibility in the
28
29 densely collapsed globule. For comparison, we can anticipate for a fully extended protein, e.g.,
30
31 denatured with 8 M urea, of the same length as MAX a ^{15}N - T_1 on the order of 1 s^{7,10} due to the
32
33 faster internal dynamics in this hypothetical extended polypeptide. Surprisingly, for the dimer
34
35 transverse relaxation times of ^{15}N - $T_2 > 1.5$ s (at 14.1 T) have been reported, which are
36
37 astonishingly long.⁵ However, the authors of this study suggest that these values are to be
38
39 analyzed with caution due to the strongly anisotropic rotation of MAX₂, which might introduce
40
41 significant biases. Yet, the short ^{15}N - T_1 for the intrinsically disordered state in comparison to the
42
43 ^{15}N - T_1 of the dimer corroborates the idea of reduced flexibility and, hence, compactness of the
44
45 monomeric state.
46
47
48
49
50
51
52
53
54
55
56
57
58
59
60

1
2
3 In Fig. 6b ^{15}N - T_2 values are shown. As for ^{15}N - T_1 , it can be observed that ^{15}N - T_2 values are on
4 average rather short for an IDP, especially between aa 20 and 85 spanning the $\text{H}_1\text{LH}_2/\text{LZ}$ domain
5 where we find an average ^{15}N - T_2 of 0.15 s. However, while ^{15}N - T_1 is not influenced by any
6 exchange contributions, ^{15}N - T_2 values are. Consequently, to separate the intrinsic relaxation from
7 the exchange contribution we detected ^{15}N - $T_{2,0}$ values in the presence of a 1 kHz CPMG field,
8 which suppresses the exchange contribution. Fig. 6c displays the ^{15}N - $T_{2,0}$ data showing that ^{15}N -
9 $T_{2,0}$ amounts on average to 0.24 s in the region spanning the $\text{H}_1\text{LH}_2/\text{LZ}$ domain (aa 20-85), which
10 is significantly longer than ^{15}N - T_2 . The conformational exchange observed via CPMG RD thus
11 appears to primarily affect the $\text{H}_1\text{LH}_2/\text{LZ}$ motif in accordance with the observation of strong
12 relaxation dispersion in this area (see the Experimental section). The $\text{H}_1\text{LH}_2/\text{LZ}$ region folds
13 upon homodimerization and constitutes the anchor between the two monomer units and thus
14 enables the formation of the coiled-coil motif. Such, the conformational exchange between
15 folded and unfolded state shortens the effective transverse relaxation times leading to the
16 observed CPMG profiles. Note that for both, ^{15}N - $T_{2,0}$ and ^{15}N - T_2 , the residue-resolved profiles
17 are quite flat between aa 20 and 85 indicating like ^{15}N - T_1 the absence of significant local
18 structures in the collapsed globule.
19
20
21
22
23
24
25
26
27
28
29
30
31
32
33
34
35
36
37
38
39
40
41

42 Furthermore, it should be noted that an average ^{15}N - $T_{2,0}$ of 0.24 s is again at the lower edge of the
43 spectrum of possible transverse relaxation times expected for an IDP. For an IDP of the size of
44 MAX one would expect values between 0.25 and 0.5 s,^{7, 26, 30-31} such that a value of 0.24 s
45 indicates a high degree of compactness and a consequent restriction of local dynamics that
46 reduces relaxation times. For the dimer an average ^{15}N - T_2 of only ~ 0.04 s has been reported.⁵
47 This value is very short in comparison to the reported ^{15}N - T_1 of > 1.5 s due to the strongly
48 anisotropic rotation and rigidity of the dimer and therefore needs to be analyzed with caution.
49
50
51
52
53
54
55
56
57
58
59
60

1
2
3 It should be noted that from the average value of $^{15}\text{N-T}_{2,0}/^{15}\text{N-T}_1$ an average rotational correlation
4 time of 1.7 ns can be estimated via the relation $\tau_c = (6^{15}\text{N-T}_{2,0}/^{15}\text{N-T}_1 - 7)^{1/2}/4\pi\nu(^{15}\text{N})$ (see
5 reference ³²) under the assumption of a simple spherical rotation for the spectral density function,
6 while we found 1.6 ns via our TRACT experiments using the same model (see the Experimental
7 section) indicating the consistency of the NMR data. However, from the hydrodynamic radius
8 obtained via PFG-DOSY for the intrinsically disordered state a significantly larger value of
9 8.3 ± 2.6 ns can be determined using the hydrodynamic relation for hard spheres $\tau_c = 4\pi\eta R_h^3/3kT$.
10 This discrepancy between the value obtained from PFG-DOSY or from relaxation times
11 indicates that a simple spherical model is not suited for a precise description (neither
12 hydrodynamic nor spectroscopic) of the dynamics of IDPs. Instead the hard sphere model serves
13 here only as a simplest tool to obtain a rough estimate of correlation times in the low ns range. At
14 present, no model exists that accurately considers all aspects of IDP dynamics and the deduction
15 of more complex models for the description of MAX is beyond the scope of this work. Currently,
16 we are working on a detailed analysis of the relaxation data with more sophisticated dynamics
17 models
18
19
20
21
22
23
24
25
26
27
28
29
30
31
32
33
34
35
36
37
38
39

40 Finally, we determined heteronuclear $^{15}\text{N}\{-^1\text{H}^{\text{N}}\}$ Overhauser enhancements (NOE, η) as a
41 function of residue position (see Fig. 6d). η is indicative for fast backbone vibrations on the
42 picosecond time scale. Such vibrations have been observed to be important for substrate
43 interactions in IDPs.⁷ In a simplified picture, positive values can be interpreted as slow
44 fluctuations on this time scale, while negative values indicate the opposite. We find positive
45 values with $0 < \eta < 0.5$ for the largest part of the backbone spanning the entire b/H₁LH₂/LZ
46 domain indicating the absence of fast vibrations on the picoseconds time scale in this region.
47 Only a few values with $\eta > 0.5$ could be observed around position 50. Negative NOEs could be
48
49
50
51
52
53
54
55
56
57
58
59
60

1
2
3 observed at the C-terminus due to its intrinsically high motional freedom. The overall flat NOE
4 profile in Fig. 6d implies homogeneous internal dynamics of the collapsed globule of the MAX
5 monomer, which is in good agreement with the flat $^{15}\text{N-T}_{2,0}$ and $^{15}\text{N-T}_1$ profiles that are
6 representative for ns-timescale motions. Note that the polymer physical model of a collapsed
7 globule likewise assumes the absence of any structural element and thus predicts a
8 homogeneous, i.e., a self-similar (fractal) internal configuration of the polypeptide chain.
9
10
11
12
13
14
15
16

17
18 This match between our NMR data and the simple polymer physical model is interesting in
19 regard of the frequent observation that IDP dynamics take place on a range of different
20 timescales and cannot be described by simple models (as evident from the PFG-DOSY data).
21 Instead, the assumption of a distribution of different correlation times for the different time
22 regimes appears to be necessary to describe IDP dynamics.²⁶⁻²⁷ For the case of MAX, the
23 homogeneous η , $^{15}\text{N-T}_{2,0}$ and $^{15}\text{N-T}_1$ profiles in Fig. 6 suggest that the distribution of correlation
24 times is quite constant for the different positions along the polypeptide chain since a variation of
25 the latter would cause residue position-dependent variations for at least one relaxation
26 parameter.
27
28
29
30
31
32
33
34
35
36
37
38
39

40 CONCLUSION

41
42
43 Summing up, the PRE profiles in Fig. 3 supplemented with DOSY as well as T_1 , T_2 and NOE
44 data indicate the presence of a strongly compacted state spanning the $\text{H}_1\text{LH}_2/\text{LZ}$ domain of the
45 intrinsically disordered state of MAX. The formation of this strongly compacted structure might
46 be involved in the conformational transition between the folded and disordered states of MAX
47 since it spans the $\text{H}_1\text{LH}_2/\text{LZ}$ domain which constitutes the central structural motif of the MAX_2
48 dimer and the anchor point between the two unimer units. It has been reported along these lines
49
50
51
52
53
54
55
56
57
58
59
60

1
2
3 that strongly compacted states of IDPs can either serve to aid subsequent folding by reducing the
4 loss in configurational entropy upon folding³³ or to prevent the formation of secondary/tertiary
5 structures by increasing the internal friction within the polypeptide chain.²³
6
7
8
9

10
11 Such, folded globular proteins cannot unhesitatingly be considered as the compact counterpart of
12 IDPs. The here observed compact conformation of the monomeric form of the Myc-associated
13 factor X is, to the best of our knowledge, the most compact IDP conformation with a degree of
14 compression comparable to folded proteins. This hints towards the importance of compacted, yet
15 unfolded structures in heterogeneous conformational spaces of IDPs.
16
17
18
19
20
21
22
23
24
25
26

27 ASSOCIATED CONTENT

28
29
30
31 **Supporting Information.** CPMG RD Data, NMR Resonance Assignment
32
33

34 AUTHOR INFORMATION

35 36 37 **Corresponding Author**

38 DK, email: kurzbach@ens.fr phone: +33 1 44323265
39
40
41
42

43 **Author Contributions**

44
45 The manuscript was written through contributions of all authors. All authors have given approval
46 to the final version of the manuscript. ‡These authors contributed equally.
47
48
49
50

51 **Funding Sources**

52
53
54
55
56
57
58
59
60

1
2
3 DK acknowledges a Feodor Lynen scholarship by the Alexander von Humboldt-Foundation.
4
5 This work was supported by the Austrian Science Foundation (FWF) (W1221 and I844) and by
6
7 the European Research Council (ERC contract ‘dilute para water’).
8
9

10 ACKNOWLEDGMENT

11
12
13
14 The authors want to thank Prof. Robert Konrat and Prof. Geoffrey Bodenhausen for granting
15
16 access to their laboratories.
17
18
19

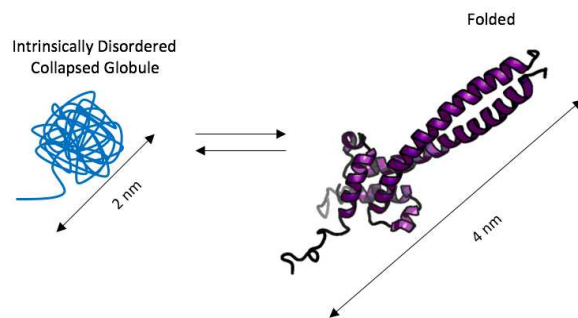
20 REFERENCES

- 21
22 1. Blackwood, E. M.; Eisenman, R. N., Max - a Helix-Loop-Helix Zipper Protein That
23 Forms a Sequence-Specific DNA-Binding Complex with Myc. *Science* **1991**, *251*, 1211-1217.
24
- 25 2. Littlewood, T. D.; Amati, B.; Land, H.; Evan, G. I., Max and C-Myc Max DNA-Binding
26 Activities in Cell-Extracts. *Oncogene* **1992**, *7*, 1783-1792.
27
- 28 3. Conacci-Sorrell, M.; McFerrin, L.; Eisenman, R. N., An Overview of MYC and Its
29 Interactome. *Csh. Perspect. Med.* **2014**, *4*, 1-24.
30
- 31 4. Sauve, S.; Tremblay, L.; Lavigne, P., The NMR solution structure of a mutant of the max
32 b/HLH/LZ free of DNA: Insights into the specific and reversible DNA binding mechanism of
33 dimeric transcription factors. *J. Mol. Biol.* **2004**, *342*, 813-832.
34
- 35 5. Brownlie, P.; Ceska, T. A.; Lamers, M.; Romier, C.; Stier, G.; Teo, H.; Suck, D., The
36 crystal structure of an intact human Max-DNA complex: New insights into mechanisms of
37 transcriptional control. *Structure* **1997**, *5*, 509-520.
38
- 39 6. Fieber, W.; Schneider, M. L.; Matt, T.; Krautler, B.; Konrat, R.; Bister, K., Structure,
40 function, and dynamics of the dimerization and DNA-binding domain of oncogenic transcription
41 factor v-Myc. *J. Mol. Biol.* **2001**, *307*, 1395-1410.
42
- 43 7. Kurzbach, D.; Schwarz, T. C.; Platzer, G.; Höfler, S.; Hinderberger, D.; Konrat, R.,
44 Compensatory Adaptations of Structural Dynamics in an Intrinsically Disordered Protein
45 Complex. *Angew. Chem. Int. Ed.* **2014**, *53*, 3840-3843.
46
- 47 8. Babu, M. M.; van der Lee, R.; de Groot, N. S.; Gsponer, J., Intrinsically disordered
48 proteins: regulation and disease. *Curr. Opinion Struct. Biol.* **2011**, *21*, 432-440.
49
- 50 9. Panchal, S. C.; Bhavesh, N. S.; Hosur, R. V., Improved 3D triple resonance experiments,
51 HNN and HN(C)N, for H-N and N-15 sequential correlations in (C-13, N-15) labeled proteins:
52 Application to unfolded proteins. *J. Biomol. NMR* **2001**, *20* (2), 135-147.
53
- 54 10. Rule, G. S.; Hitchens, T. K., *Fundamentals of Protein NMR Spectroscopy*. Springer:
55 Dordrecht, 2006.
56
57
58
59
60

11. Korzhnev, D. M.; Kay, L. E., Probing invisible, low-populated states of protein molecules by relaxation dispersion NMR spectroscopy: An application to protein folding. *Accounts Chem. Res.* **2008**, *41*, 442-451.
12. Carver, J. P.; Richards, E. R., A General Two-Site Solution for the Chemical Exchange Produced Dependence of T2 Upon Carr-Purcell Pulse Separation. *J. Magn. Reson.* **1972**, *6*, 89-105.
13. Luz, Z.; Meiboom, S., Nuclear Magnetic Resonance Study of the Protolysis of Trimethylammonium Ion in Aqueous Solution-Order of the Reaction with Respect to Solvent. *J. Chem. Phys.* **1963**, *39*, 366-370.
14. Battiste, J. L.; Wagner, G., Utilization of site-directed spin labeling and high-resolution heteronuclear nuclear magnetic resonance for global fold determination of large proteins with limited nuclear overhauser effect data. *Biochemistry* **2000**, *39*, 5355-5365.
15. Clore, G. M.; Iwahara, J., Theory, Practice, and Applications of Paramagnetic Relaxation Enhancement for the Characterization of Transient Low-Population States of Biological Macromolecules and Their Complexes. *Chem. Rev.* **2009**, *109*, 4108-4139.
16. Wilkins, D. K.; Grimshaw, S. B.; Receveur, V.; Dobson, C. M.; Jones, J. A.; Smith, L. J., Hydrodynamic radii of native and denatured proteins measured by pulse field gradient NMR techniques. *Biochemistry* **1999**, *38*, 16424-16431.
17. Nilsson, M., The DOSY Toolbox: a new tool for processing PFG NMR diffusion data. *J. Magn. Reson.* **2009**, *200*, 296-302.
18. Lee, D.; Hilty, C.; Wider, G.; Wuthrich, K., Effective rotational correlation times of proteins from NMR relaxation interference. *J. Magn. Reson.* **2006**, *178*, 72-76.
19. Kurzbach, D.; Platzer, G.; Schwarz, T. C.; Henen, M. A.; Konrat, R.; Hinderberger, D., Cooperative Unfolding of Compact Conformations of the Intrinsically Disordered Protein Osteopontin. *Biochemistry* **2013**, *52*, 5167-5175.
20. Platzer, G.; Schedlbauer, A.; Chemelli, A.; Ozdowy, P.; Coudeville, N.; Auer, R.; Kontaxis, G.; Hartl, M.; Miles, A. J.; Wallace, B. A.; Glatter, O.; Bister, K.; Konrat, R., The Metastasis-Associated Extracellular Matrix Protein Osteopontin Forms Transient Structure in Ligand Interaction Sites. *Biochemistry* **2011**, *50*, 6113-6124.
21. Geist, L.; Henen, M. A.; Haiderer, S.; Schwarz, T. C.; Kurzbach, D.; Zawadzka-Kazimierczuk, A.; Saxena, S.; Zerko, S.; Kozminski, W.; Hinderberger, D.; Konrat, R., Protonation-dependent conformational variability of intrinsically disordered proteins. *Protein Science* **2013**, *22*, 1196-1205.
22. Nettels, D.; Muller-Spath, S.; Kuster, F.; Hofmann, H.; Haenni, D.; Ruegger, S.; Reymond, L.; Hoffmann, A.; Kubelka, J.; Heinz, B.; Gast, K.; Best, R. B.; Schuler, B., Single-molecule spectroscopy of the temperature-induced collapse of unfolded proteins. *Proc. Nat. Acad. Sci.* **2009**, *106*, 20740-20745.
23. Soranno, A.; Buchli, B.; Nettels, D.; Cheng, R. R.; Muller-Spath, S.; Pfeil, S. H.; Hoffmann, A.; Lipman, E. A.; Makarov, D. E.; Schuler, B., Quantifying internal friction in unfolded and intrinsically disordered proteins with single-molecule spectroscopy. *Proc. Nat. Acad. Sci.* **2012**, *109*, 17800-17806.

- 1
2
3
4
5
6
7
8
9
10
11
12
13
14
15
16
17
18
19
20
21
22
23
24
25
26
27
28
29
30
31
32
33
34
35
36
37
38
39
40
41
42
43
44
45
46
47
48
49
50
51
52
53
54
55
56
57
58
59
60
24. Aznauryan, M.; Nettels, D.; Holla, A.; Hofmann, H.; Schuler, B., Single-Molecule Spectroscopy of Cold Denaturation and the Temperature-Induced Collapse of Unfolded Proteins. *J. Am. Chem. Soc.* **2013**, *135*, 14040-14043.
 25. Rubinstein, M.; Colby, R., *Polymer Physics*. Oxford University Press: 2003.
 26. Khan, S. N.; Charlier, C.; Augustyniak, R.; Salvi, N.; Dejean, V.; Bodenhausen, G.; Lequin, O.; Pelupessy, P.; Ferrage, F., Distribution of Pico- and Nanosecond Motions in Disordered Proteins from Nuclear Spin Relaxation. *Biophys. J.* **2015**, *109*, 988-999.
 27. Charlier, C.; Khan, S. N.; Marquardsen, T.; Pelupessy, P.; Reiss, V.; Sakellariou, D.; Bodenhausen, G.; Engelke, F.; Ferrage, F., Nanosecond time scale motions in proteins revealed by high-resolution NMR relaxometry. *J. Am. Chem. Soc.* **2013**, *135*, 18665-18672.
 28. Kurzbach, D.; Beier, A.; Vanas, A.; Flamm, A. G.; Platzer, G.; Schwarz, T. C.; Konrat, R., NMR probing and visualization of correlated structural fluctuations in intrinsically disordered proteins. *Phys, Chem, Chem, Phys*, **2017**, *19*, 10651-10656.
 29. Konrat, R., The meandering of disordered proteins in conformational space. *Structure* **2010**, *18*, 416-419.
 30. Salvi, N.; Abyzov, A.; Blackledge, M., Multi-Timescale Dynamics in Intrinsically Disordered Proteins from NMR Relaxation and Molecular Simulation. *J. Phys. Chem. Lett.* **2016**, *7* (13), 2483-2489.
 31. De Biasio, A.; de Opakua, A. I.; Cordeiro, T. N.; Villate, M.; Merino, N.; Sibille, N.; Lelli, M.; Diercks, T.; Bernado, P.; Blanco, F. J., p15(PAF) Is an Intrinsically Disordered Protein with Nonrandom Structural Preferences at Sites of Interaction with Other Proteins. *Biophys. J.* **2014**, *106*, 865-874.
 32. Kay, L. E.; Torchia, D. A.; Bax, A., Backbone dynamics of proteins as studied by ¹⁵N inverse detected heteronuclear NMR spectroscopy: application to staphylococcal nuclease. *Biochemistry* **1989**, *28*, 8972-8979.
 33. Cheung, J. K.; Shah, P.; Truskett, T. M., Heteropolymer collapse theory for protein folding in the pressure-temperature plane. *Biophys. J.* **2006**, *91*, 2427-2435.

For Table of Contents Use Only



1
2
3
4
5
6
7
8
9
10
11
12
13
14
15
16
17
18
19
20
21
22
23
24
25
26
27
28
29
30
31
32
33
34
35
36
37
38
39
40
41
42
43
44
45
46
47
48
49
50
51
52
53
54
55
56
57
58
59
60